

Inflation model of Uzon caldera, Kamchatka, constrained by satellite radar interferometry observations

Paul Lundgren¹ and Zhong Lu²

Received 14 November 2005; revised 26 January 2006; accepted 31 January 2006; published 16 March 2006.

[1] We analyzed RADARSAT-1 synthetic aperture radar (SAR) data to compute interferometric SAR (InSAR) images of surface deformation at Uzon caldera, Kamchatka, Russia. From 2000 to 2003 approximately 0.15 m of inflation occurred at Uzon caldera, extending beneath adjacent Kikhpinych volcano. This contrasts with InSAR data showing no significant deformation during either the 1999 to 2000, or 2003 to 2004, time periods. We performed three sets of numerical source inversions to fit InSAR data from three different swaths spanning 2000 to 2003. The preferred source model is an irregularly shaped, pressurized crack, dipping $\sim 20^\circ$ to the NW, 4 km below the surface. The geometry of this solution is similar to the upper boundary of the geologically inferred magma chamber. Extension of the surface deformation and source to adjacent Kikhpinych volcano, without an eruption, suggests that the deformation is more likely of hydrothermal origin, possibly driven by recharge of the magma chamber. **Citation:** Lundgren, P., and Z. Lu (2006), Inflation model of Uzon caldera, Kamchatka, constrained by satellite radar interferometry observations, *Geophys. Res. Lett.*, 33, L06301, doi:10.1029/2005GL025181.

1. Introduction

[2] One of the most active volcanic arcs in the Pacific Rim, Kamchatka is also one with poor geophysical constraints on its shallow magma plumbing systems. Uzon caldera (Figure 1) lies within a graben approximately 20 km wide running beneath the eastern Kamchatka volcanic group [Belousov *et al.*, 1984; Leonov, 2000]. Cross sections of the shallow crustal graben show that it steps WNW from its southeasterly bounding fault beneath Kikhpinych volcano, deepening toward Uzon caldera. The Valley of the Geysers in the far eastern portion of Uzon caldera is considered derived from shallow meteoric water in contact with a heat source associated with Kikhpinych volcano [Belousov *et al.*, 1984; Leonov *et al.*, 1991]. The general structure hypothesized by Belousov *et al.* [1984] places a deep aquifer shallower than a depth of about 2 km with the top of a cooling magma chamber at depths greater than 4 km from beneath the eastern side of the caldera complex, to over 10 km toward its western end. Geological observations of extruded lavas and other deposits over the course of Uzon's history show that there have been episodic

basalt intrusions into a granitic magma chamber, with the system becoming progressively more crystallized and lower in temperature with time [Belousov *et al.*, 1984].

[3] We analyzed RADARSAT-1 data from 1999 through 2004 and found that from 2000 to 2003 (there are no data in 2002) Uzon caldera inflated with an amplitude of nearly 15 cm in the satellite line-of-sight (LOS). We modeled this data with a series of methods that seek to define both its gross geometry, and subsequently, the more complex source geometry that is required to fit the observed deformation pattern.

2. InSAR Analysis

[4] We analyzed SAR data from the RADARSAT-1 satellite (Figure 2) using the ROI_PAC software package developed at JPL/Caltech. This includes the standard removal of topographic effects using simulations based on the Shuttle Radar Topography Mission (SRTM) 90-m digital elevation data, and re-estimation of the baselines of each interferogram [Rosen *et al.*, 2000].

[5] Significant deformation is found for the period spanning 2000 to 2003 (Figures 2a, 2c, and 2f), whereas from 1999 to 2000 (Figure 2e), and from 2003 to 2004 (Figure 2g), we found no significant deformation. The partial coverage shown in Figure 2f is the same InSAR data shown by Pritchard and Simons [2004]. As indicated in Figure 2, these data are from different swaths and have different ground incidence angles. Independent interferograms from different swaths and different dates show very similar deformation patterns and amplitudes, despite often significant atmospheric artifacts and problems with residual ramps due to imperfect baseline re-estimation. In particular, topographically correlated atmospheric phase is evident, which either adds to (Figure 2c) or subtracts from (Figures 2a, 2b, and 2d) the caldera deformation in areas of higher topography around Kikhpinych volcano. We found an irregular, smoothly varying pattern of positive LOS movement with a peak amplitude of approximately 15 cm for the period 2000 to 2003.

3. Modeling

[6] The shape of the surface deformation requires a source that produces only positive LOS displacements. A lack of a generally circular, concentric pattern, as has been observed for a number of other Aleutian volcanoes [Lu *et al.*, 2003], suggests that a spherically symmetric pressure source is not the answer. Also, a lack of significant SW-NE complexity in the fringe pattern does not suggest shear faulting as the source. This leaves a tabular pressure source as the simplest starting model, although this may be thought

¹Jet Propulsion Laboratory, California Institute of Technology, Pasadena, California, USA.

²Science Applications International Corporation, U.S. Geological Survey Center for EROS, Sioux Falls, South Dakota, USA.

of as a simplification for a volume source with a deeper vertical root, to which the surface deformation is relatively insensitive [Yun *et al.*, 2006]. The steep gradient in phase cycles (fringes) along the deformation pattern's eastern edge is inconsistent with a point source and suggests that the source is shallower to the southeast (deeper to the NW). However, this gradient is not so steep as to require passive slip along the caldera boundary [De Natale *et al.*, 1997; Amelung *et al.*, 2000]. The 'coma' shaped pattern, with the largest amplitude representing the 'head' of the coma and the 'tail' trending to the west, suggests some geometrical complexity to the source.

[7] We modeled the deformation for the three independent 2000–2003 interferograms shown in Figures 2a, 2c, and 2f. These interferograms are for RADARSAT-1 beams 7, 4, and 6, respectively, with incidence angles (from vertical) of approximately 48°, 38°, and 42° over the caldera for each of the respective interferograms. These incidence angles are nearly as sensitive to horizontal as to vertical displacements in the range direction (to the WNW). To reduce model sensitivity to broad, long wavelength signal in the interferogram, which is more susceptible to atmospheric noise, while maintaining relatively higher data density in the areas of higher geophysical signal, we down-sampled the data using a version of the quadtree partitioning algorithm of Jonsson *et al.* [2002]. We applied this to data within coherence masks defined by the interferogram unwrapper snaphu [Chen and Zebker, 2001]. This down-sampling resulted in 623, 507, and 228 data points in 2a, 2c, and 2f, respectively (Figure 3a). As a first step we solved for the best-fitting tensile dislocation using a Levenberg-Marquardt nonlinear least squares inversion [Lundgren *et al.*, 2003]. We tested a range of forward models to find a reasonable starting location and geometry, since this type of inversion is sensitive to the starting model. We solved for the location (x, y, z), length, width, dip, and tensile (u_3) displacement, constraining the strike to 210° and the shear displacements to zero. The resulting solution is a dislocation approximately 8.7×15.4 km, dipping 19° to the NW, starting from a depth of 3.1 km, with a displacement of 0.27 m. The modeled surface displacements in the LOS provide a reasonable fit to the observed InSAR displacements, though without fitting the details of the higher displacement areas (Figure 3b). A map-

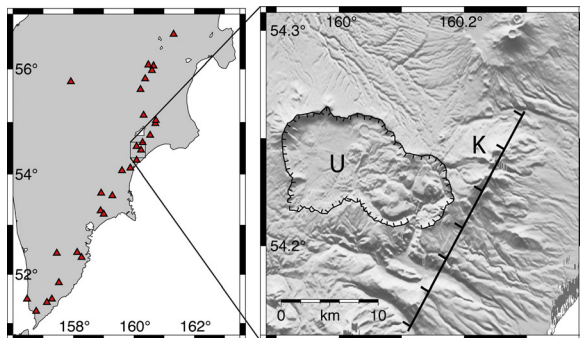


Figure 1. (a) Location map of Uzon caldera with active Kamchatkan volcanoes shown as red triangles. (b) Shaded relief map of the SRTM digital elevation model covering the same area as shown in Figures 2a–2d, 3, and 4. The closed hatched line shows the caldera boundary. U is Uzon caldera, K, Kikhpinych volcano. The linear hatched line indicates the SE side of the graben.

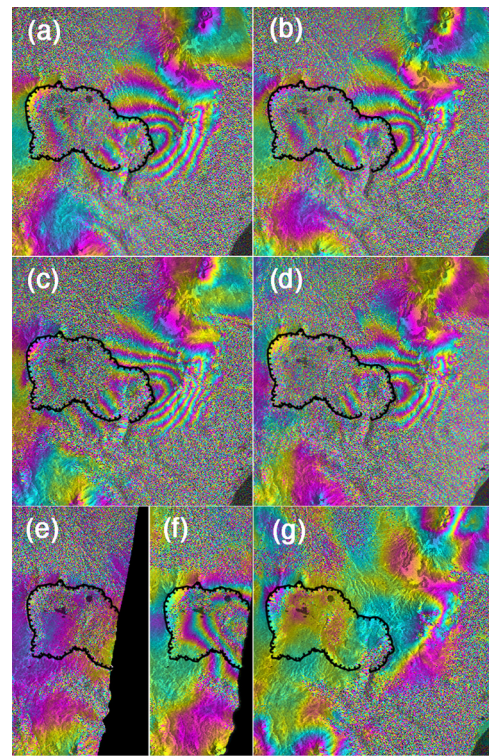


Figure 2. SAR interferograms, each color cycle represents 2.8 cm of LOS surface displacement. Hatched lines indicate the caldera rim. For each interferogram shown we indicate the dates of the SAR images, the perpendicular baselines, and the RADARSAT-1 beam and its surface incidence angle at the Uzon caldera. (a) 2000/08/23–2003/08/08. Bp = –54. Beam 7 (48°). (b) 2000/08/23–2004/09/19. Bp = 176. Beam 7 (48°). (c) 2000/09/19–2003/08/11. Bp = –58. Beam 4 (38°). (d) 2000/09/16–2004/08/02 Bp = 126. Beam 7 (48°). (e) 1999/09/08–2000/09/02. Bp = 483. Beam 6 (42°). (f) 2000/09/02–2003/08/18. Bp = 218. Beam 6 (42°). (g) 2003/09/04–2004/08/05. Bp = 80. Beam 4 (38°).

view of the solution is the interior 80% of the rectangular area shown in Figure 4a. Model misfit and the estimated phase shifts for each modeled interferogram are given in Table S1.¹

[8] In the next step, we took the solution from the nonlinear inversion, extended its area by 10% from each edge [Pedersen and Sigmundsson, 2004], and divided it into a 10×10 grid of dislocations. We applied a non-negative least squares inversion with a tunable smoothing factor, as described by Jonsson *et al.* [2002]. Figure S1 shows the misfit versus solution roughness curve as a function of the smoothing parameter. We used a value of 20, near the 'corner' in the curve, where increased solution roughness does not lead to significant reduction in error. The resulting synthetic LOS displacements and slip model are shown in Figures 3c and 4a, respectively. Because of the tradeoff in patch size (number of patches) and depth, the inversion was not sensitive to depth in the 2–5 km depth range. Therefore, we left the solution depth at the single dislocation depth (2.5 km to the top edge of the extended source plane). As might be expected, the opening is largest along a diagonal

¹Auxiliary material is available at <ftp://ftp.agu.org/apend/gl/2005gl025181>.

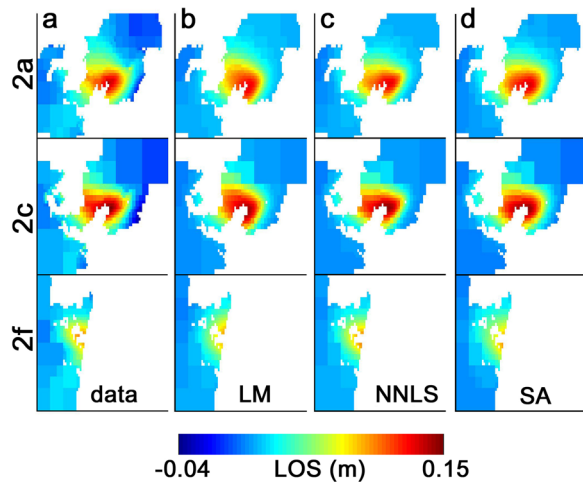


Figure 3. Observed and modeled LOS surface displacements from the three modeled interferograms shown in Figures 2a, 2c, and 2f and quadtree averaged as indicated in the text. (a) Observed data. (b) Modeled deformation for the best-fitting single tensile dislocation source. (c) Smoothed non-negative least-squares solution. (d) Simulated annealing tensile crack solution.

from the down-dip SW corner to the up-dip NE corner of the fault plane, with a maximum opening of over 0.5 m. Not surprisingly, the distributed opening solution provides a significant reduction in model misfit (see Table S1).

[9] We next used the same 10×10 patch plane to solve for the best fitting pressurized crack. This solution requires fewer free parameters and would allow for a more physical description of the source that could be used to assess the resulting stress changes and their effects on dike propagation or slip on nearby structures. To achieve this we used a simulated annealing algorithm to define the crack as a randomly selected set of patches [Yun *et al.*, 2006]. To calculate the forward crack solution for each configuration of patches, we used POLY3D, a boundary element solution program for arbitrary polygonal elements in an elastic half-space [Thomas, 1993]. Unlike the dislocation inversions, the simulated annealing solution is more computationally intensive, since each crack solution is unique and each trial model requires a new POLY3D solution.

[10] We solved over a range of depths (from 2–6 km) in 0.5 km increments. The resulting minimum error was found for a depth of 4 km, although solutions at 3.5 and 4.5 had similar errors, whereas away from this depth range the misfit increased rapidly. The solution where the depth to the upper edge of the extended crack is 4 km is shown in Figure 4b, and the synthetic LOS surface displacements in Figure 3d. The excess pressure change is 1.6 MPa, using a Young's modulus of 30 GPa, with a maximum patch center displacement of 0.57 m.

4. Discussion and Conclusions

[11] A comparison of the pressurized crack solution (Figure 4b) and the general structure postulated by Belousov *et al.* [1984] is shown in Figure 4c. The InSAR based solution agrees remarkably well with the hypothesized structure and the deepening of the magma system to the NW. If our

solution is referenced to the ~ 1 km surface topographic height of Uzon caldera, then our modeled source should be shifted by approximately 1 km to shallower depth. This would still leave the deformation source in close proximity to the proposed magma chamber, and is at odds with a hydrothermal system shallower than 2 km as the deformation source.

[12] In other caldera systems such as Campi Flegrei, Long Valley, and Yellowstone, inflation has been observed without subsequent short-term eruptions [Battaglia *et al.*, 1999]. In the case of Campi Flegrei, large (1.5 m) uplift in less than a year has been modeled as amplification of a deep seated (>4 km) magma system either through the ring fault system [De Natale *et al.*, 1997] or through hydrothermal effects in the caldera fill [Gaeta *et al.*, 1998; Orsi *et al.*, 1999]. Yellowstone has experienced spatiotemporally varying deformation interpreted as a linked hydrothermal system [Wicks *et al.*, 1998]. In the case of Uzon caldera, the InSAR deformation is not so large that it requires hydrothermal amplification to avoid unnecessarily large over pressures if the source were greater than 4 km depth, nor does the deformation pattern show effects that suggest there is shallow ring-fault motion (see Figures S2 and S3 for comparison). This suggests that the simplest explanation for this deformation is linked to a magma source, either directly, or through hydrothermal fluids trapped immediately above the magma chamber such that these fluids follow the general deepening of the magma chamber to the NW. The pressure change we estimate (1.6 MPa) is relatively small and dependent on the spatial extent of the modeled crack. Its relatively low amplitude does not favor either a magmatic or hydrothermal source.

[13] The general picture that emerges (Figures 4b and 4c) suggests a complex source that, at least within the temporal resolution of our InSAR data (during 2000 to 2003), must be both heterogeneous yet interconnected. The main regions of uplift occur beneath central and eastern Uzon caldera, with extension beyond the caldera to the NE beneath Kikhpinych volcano and bounded to the ESE by the graben

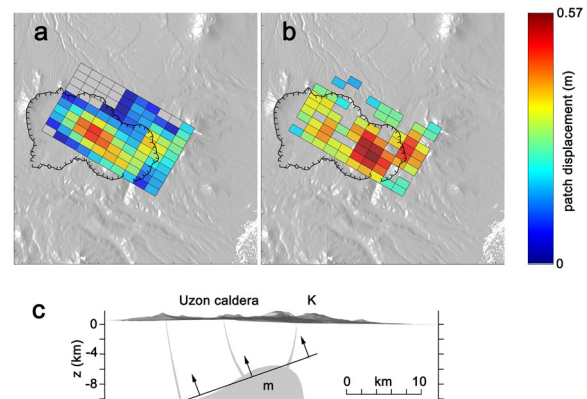


Figure 4. Map views of the modeled solutions. (a) Distributed tensile opening non-negative least-squares solution at a half-space depth of 2.5 km, dip 19° to the NW, over the dislocation geometry obtained for the single dislocation inversion, extended by 20% in length and width. (b) Distributed crack solution, for a constant over pressure of 1.6 MPa at an up-dip half-space depth of 4 km. (c) Side view of the solution in Figure 4b with the approximate magma chamber (*m*) and fault and conduit structures given by Belousov *et al.* [1984]. *K* - Kikhpinych volcano.

bounding fault system, over which lies Kikhpinych. In the SAR interferograms, the northeastern fringes become more acute around Kikhpinych volcano, suggesting extension of the deformation source to beneath the volcano. The northeastern corner of the modeled source lies beneath Kikhpinych volcano. This would suggest a hydrothermal connection since Kikhpinych last erupted 600 years ago [Braitseva *et al.*, 1991].

[14] There are fundamental limitations to our modeling, both in terms of the data (only one look direction and three incidence angles spanning 10° , and some amount of atmospheric noise that mostly affects the longer wavelength deformation) and the modeling (elastic half-space with a limited solution space). If we had data from both ascending and descending tracks we could better constrain the source and allow resolution of the fault into smaller patches for the crack model [Lundgren *et al.*, 2003; Yun *et al.*, 2006]. This could help resolve features such as the northern edge of the pressure source and the nature of its relation to Kikhpinych volcano. Finally, the assumption that the crack opens at constant over-pressure may not be true.

[15] This study shows that analysis of RADARSAT-1 SAR data for Uzon caldera yields observations of positive LOS displacements during the 2000 to 2003 time period, with no significant deformation in each of the years before and after. We model the deformation source as a heterogeneous, interconnected set of cracks with an over-pressure of 1.6 MPa, along a plane dipping 19° toward the NW, approximately 4 km below the caldera surface, which has a mean elevation of approximately 1 km. The close proximity of this source with geologic estimates of the graben structure and solidifying magma chamber does not distinguish between either the magma chamber itself or an overlying hydrothermal origin as the source of the deformation. The heterogeneity of the source structure and its apparent connection to deformation around adjacent Kikhpinych volcano suggests a hydrothermal system linked to the underlying magma system. The variability of the deformation during the 1999 to 2004 time period shows that further observations are required to better constrain the source mechanism and its temporal behavior.

[16] **Acknowledgments.** RADARSAT-1 data are copyrighted by the Canadian Space Agency, and were provided courtesy of the Alaska Satellite Facility. We wish to thank G. De Natale and an anonymous reviewer for their insightful reviews, and S. Jonsson for his quadtree program. This research was carried out at the Jet Propulsion Laboratory, California Institute of Technology, under a contract with the National Aeronautics and Space Administration. Lu was supported by the U.S. Geological Survey Volcano Hazards Program and Land Remote Sensing Program.

References

Amelung, F., S. Jonsson, H. Zebker, and P. Segall (2000), Widespread uplift and "trapdoor" faulting on Galapagos volcanoes observed with radar interferometry, *Nature*, 407, 993–996.

- Battaglia, M., C. Roberts, and P. Segall (1999), Magma intrusion beneath Long Valley Caldera confirmed by temporal changes in gravity, *Science*, 285, 2119–2122.
- Belousov, V. I., E. N. Grib, and V. L. Leonov (1984), The geological setting of the hydrothermal systems in the Geysers Valley and Uzon caldera, *Volcanol. Seismol.*, 5, 67–81.
- Braitseva, O. A., I. V. Florensky, and O. N. Volynets (1991), Kikhpinych volcano, in *Active Volcanoes of Kamchatka*, edited by S. A. Fedotov and Y. P. Masurenkov, pp. 72–91, Nauka, Moscow.
- Chen, C. W., and H. A. Zebker (2001), Two-dimensional phase unwrapping with use of statistical models for cost functions in non-linear optimization, *J. Opt. Soc. Am.*, 18, 338–351.
- De Natale, G., S. M. Petrazzuoli, and F. Pingue (1997), The effect of collapse structures on ground deformation in calderas, *Geophys. Res. Lett.*, 24, 1555–1558.
- Gaeta, F. S., G. De Natale, F. Peluso, G. Mastrolorenzo, D. Castagnolo, C. Troise, F. Pingue, D. G. Mita, and S. Rossano (1998), Genesis and evolution of unrest episodes at Campi Flegrei caldera: The role of thermal fluid-dynamical processes in the geothermal system, *J. Geophys. Res.*, 103, 20,921–20,933.
- Jonsson, S., H. Zebker, P. Segall, and F. Amelung (2002), Fault slip distribution of the 1999 M_w 7.1 Hector Mine, California, earthquake, estimated from satellite radar and GPS measurements, *Bull. Seismol. Soc. Am.*, 92, 1377–1389.
- Leonov, V. (2000), Regional structural positions of high temperature hydrothermal systems of Kamchatka, paper presented at World Geothermal Congress 2000, Int. Geotherm. Assoc., Beppu, Japan.
- Leonov, V. L., E. N. Grib, G. A. Karpov, V. M. Sugrobov, N. G. Sugrobova, and Z. I. Zubin (1991), Uzon caldera and Valley of Geysers, in *Active Volcanoes of Kamchatka*, edited by S. A. Fedotov and Y. P. Masurenkov, pp. 92–141, Nauka, Moscow.
- Lu, Z., et al. (2003), Interferometric synthetic aperture radar studies of Alaska volcanoes, *Earth Obs. Mag.*, 12(3), 8–18.
- Lundgren, P., P. Berardino, M. Coltelli, G. Fornaro, R. Lanari, G. Puglisi, E. Sansosti, and M. Tesauro (2003), Coupled magma chamber inflation and sector collapse slip observed with synthetic aperture radar interferometry on Mt. Etna volcano, *J. Geophys. Res.*, 108(B5), 2247, doi:10.1029/2001JB000657.
- Orsi, G., S. M. Petrazzuoli, and K. Wohletz (1999), Mechanical and thermo-fluid behaviour during unrest at the Campi Flegrei caldera (Italy), *J. Volcanol. Geotherm. Res.*, 91, 453–470.
- Pedersen, R., and F. Sigmundsson (2004), InSAR based sill model links spatially offset areas of deformation and seismicity for the 1994 unrest episode at Eyjafjallajökull volcano, Iceland, *Geophys. Res. Lett.*, 31, L14610, doi:10.1029/2004GL020368.
- Pritchard, M. E., and M. Simons (2004), Surveying volcanic arcs with satellite radar interferometry: The central Andes, Kamchatka, and beyond, *GSA Today*, 14, 4–11, doi:10.1130/1052-5173.
- Rosen, P. A., S. Hensley, I. R. Joughin, F. K. Li, S. N. Madsen, E. Rodriguez, and R. M. Goldstein (2000), Synthetic aperture radar interferometry, *Proc. IEEE*, 88, 333–382.
- Thomas, A. L. (1993), Poly3D: A three-dimensional, polygonal element, displacement discontinuity boundary element computer program with applications to fractures, faults, and cavities in the Earth's crust, M.S. thesis, 221 pp., Stanford Univ., Stanford, Calif.
- Wicks, C., Jr., W. Thatcher, and D. Dzurisin (1998), Migration of fluids beneath Yellowstone caldera inferred from satellite radar interferometry, *Science*, 282, 458–462.
- Yun, S., P. Segall, and H. Zebker (2006), Constraints on magma chamber geometry at Sierra Negra volcano, Galapagos Islands, based on InSAR observations, *J. Volcanol. Geotherm. Res.*, 150, 232–243.

Z. Lu, Science Applications International Corporation, U.S. Geological Survey Center for EROS, Sioux Falls, SD 57198, USA.

P. Lundgren, Jet Propulsion Laboratory, California Institute of Technology, Pasadena, CA 91109–8099, USA. (paul@weed.jpl.nasa.gov)